

RESEARCH

Open Access



# Dosimetric benefits of adaptive radiation therapy for patients with stage III non-small cell lung cancer

Lea Hoppen<sup>1\*</sup>, Gustavo R. Sarria<sup>2</sup>, Chung S. Kwok<sup>1</sup>, Judit Boda-Heggemann<sup>1</sup>, Daniel Buergy<sup>1</sup>, Michael Ehmann<sup>1</sup>, Frank A. Giordano<sup>1</sup> and Jens Fleckenstein<sup>1</sup>

## Abstract

**Background** Daily adaptive radiation therapy (ART) of patients with non-small cell lung cancer (NSCLC) lowers organs at risk exposure while maintaining the planning target volume (PTV) coverage. Thus, ART allows an isotoxic approach with increased doses to the PTV that could improve local tumor control. Herein we evaluate daily online ART strategies regarding their impact on relevant dose-volume metrics.

**Methods** Daily cone-beam CTs ( $1 \times n=28$ ,  $1 \times n=29$ ,  $11 \times n=30$ ) of 13 stage III NSCLC patients were converted into synthetic CTs (sCTs). Treatment plans (TPs) were created retrospectively on the first-fraction sCTs (sCT<sub>1</sub>) and subsequently transferred unaltered to the sCTs of the remaining fractions of each patient (sCT<sub>2–n</sub>) (IGRT scenario). Two additional TPs were generated on sCT<sub>2–n</sub>: one minimizing the lung-dose while preserving the D<sub>95%</sub>(PTV) (isoeffective scenario), the other escalating the D<sub>95%</sub>(PTV) with a constant V<sub>20Gy</sub>(lung<sub>ipsilateral</sub>) (isotoxic scenario).

**Results** Compared to the original TPs predicted dose, the median D<sub>95%</sub>(PTV) in the IGRT scenario decreased by  $1.6 \text{ Gy} \pm 4.2 \text{ Gy}$  while the V<sub>20Gy</sub>(lung<sub>ipsilateral</sub>) increased in median by  $1.1\% \pm 4.4\%$ . The isoeffective scenario preserved the PTV coverage and reduced the median V<sub>20Gy</sub>(lung<sub>ipsilateral</sub>) by  $3.1\% \pm 3.6\%$ . Furthermore, the median V<sub>5%</sub>(heart) decreased by  $2.9\% \pm 6.4\%$ . With an isotoxic prescription, a median dose-escalation to the gross target volume of  $10.0 \text{ Gy} \pm 8.1 \text{ Gy}$  without increasing the V<sub>20Gy</sub>(lung<sub>ipsilateral</sub>) and V<sub>5%</sub>(heart) was feasible.

**Conclusions** We demonstrated that even without reducing safety margins, ART can reduce lung-doses, while still reaching adequate target coverage or escalate target doses without increasing ipsilateral lung exposure. Clinical benefits by means of toxicity and local control of both strategies should be evaluated in prospective clinical trials.

**Keywords** Adaptive radiation therapy, stage III NSCLC, Isotoxic dose-escalation, Isoeffective organ at risk sparing

## Background

The aim of radiation therapy (RT) is to achieve a high tumor control probability (TCP) with the lowest possible normal tissue complication probability (NTCP) [1]. For patients with locally advanced non-small cell lung cancer (NSCLC) the dose limiting organs at risk (OAR) are usually lungs, heart and esophagus, which tend to develop pneumonitis [2, 3], cardiovascular toxicity [4–7], or acute esophagitis [8, 9] due to high radiation doses, respectively. Most NSCLC radiation therapies are performed

\*Correspondence:

Lea Hoppen

Lea.Hoppen@umm.de

<sup>1</sup> Department of Radiation Oncology, University Medical Center Mannheim, University of Heidelberg, Theodor-Kutzer-Ufer 1-3, 68167 Mannheim, Germany

<sup>2</sup> Department of Radiation Oncology, University Hospital Bonn, University of Bonn, Bonn, Germany



© The Author(s) 2023. **Open Access** This article is licensed under a Creative Commons Attribution 4.0 International License, which permits use, sharing, adaptation, distribution and reproduction in any medium or format, as long as you give appropriate credit to the original author(s) and the source, provide a link to the Creative Commons licence, and indicate if changes were made. The images or other third party material in this article are included in the article's Creative Commons licence, unless indicated otherwise in a credit line to the material. If material is not included in the article's Creative Commons licence and your intended use is not permitted by statutory regulation or exceeds the permitted use, you will need to obtain permission directly from the copyright holder. To view a copy of this licence, visit <http://creativecommons.org/licenses/by/4.0/>. The Creative Commons Public Domain Dedication waiver (<http://creativecommons.org/publicdomain/zero/1.0/>) applies to the data made available in this article, unless otherwise stated in a credit line to the data.

with 60–70 Gy total dose in 1.8–2 Gy-fractions [5, 10, 11]. Survival rates of patients with locally advanced (stage III) NSCLC have improved considerably during the last years. Modern concurrent chemoradiotherapy (cCRT) results in 5-year overall survival (OS) rates of 32–33% [12, 13]; results can be further improved in patients who are eligible for immunotherapy (absence of toxic events  $\geq$  grade 2) with durvalumab as a consolidation therapy resulting in 5-year OS rates of approximately 43% [13]. Despite these improvements, only one third of patients treated with cCRT or immunotherapy survives or remains free from progression five years after treatment [13].

Currently, treatment plans are typically generated on a pre-treatment computed tomography (CT) scan and delivered in all treatment fractions by means of daily image guided radiation therapy (IGRT), sometimes in combination with an active motion management concept. Intrafractional motion management is mostly realized by either an internal target volume (ITV) margin, beam tracking or gating concepts [14]. The latter two reduce the planning target volume (PTV) size and aim at a quasi-static situation. However, all these workflows ensure adequate patient positioning but neglect inter-fractional morphologic changes in the patient's anatomy which may lead to discrepancies between the delivered and planned dose [1, 15, 16]. This is of particular relevance for NSCLC since these tumors are generally early responders to radiation [16, 17]. On average the gross target volume (GTV) of NSCLC patients shrinks 0.6–2.4% per day during RT [3].

In online adaptive radiation therapy (ART), treatment plans are adjusted to a possibly changed patient anatomy [1, 15, 16] on daily pre-treatment imaging. This is mostly performed with cone-beam computed tomography (CBCT)-based approaches. Compared to fan-beam CTs, CBCTs present limitations such as, inferior image quality and lack of a unique CT-number-to-electron density calibration [18–21]. Furthermore, they have only a limited field of view (FOV) capacity, which may not enclose the structure set in its entirety. For image segmentation and dose calculation, the insufficient image quality has recently been overcome by generating synthetic CTs (sCTs) with an artificial intelligence (AI) approach [22].

The aim of ART is to minimize the discrepancies between high dose volumes and the actual clinical target volumes (CTV) and therefore, to further broaden the therapeutic window. In ART for patients with NSCLC, this can be realized with one of the following adaptation strategies: sparing the OARs while leaving the dose delivered to the PTV unaltered (isoeffective scenario) or escalating the dose to the PTV without increasing the ipsilateral lung-dose (isotoxic scenario) [16]. By

minimizing OAR-doses, the risk of toxic events can be reduced [3, 9, 23]. This increases the probability that patients will be eligible for immunotherapy [7, 24]. Several analyses showed that increased OAR-doses are associated with worse OS [4, 5, 25]. Moreover, no correlation between effect and different tumor types or locations has been yet determined. Several studies concluded that in lung cancer higher fractional doses lead to higher TCP and OS [26–28]. This was, however, questioned by the results of the RTOG-0617 study which showed that patients treated with 60 Gy had better progression-free survival (PFS) and OS rates than patients treated with 74 Gy [5]. In the 74 Gy arm higher doses to the heart, lung, and esophagus were delivered compared to the 60 Gy arm [5, 25]. Higher lung- and heart-doses were associated with worsened OS [4, 5, 25, 29], which may explain the better outcome of the 60-Gy arm. Further analysis of the patient population indicated that dose-escalation may improve OS rates for patients with radioresistant genotypes [30].

This study aims to determine the differences between planned and delivered doses. Furthermore, the maximum dosimetric benefits of isotoxic and isoeffective daily online ART approaches with deep inspiration breath-hold technique (DIBH) for target immobilization shall be determined.

## Methods

### Patient population and treatment workflow

In this retrospective treatment planning study 13 patients with stages III/IV NSCLC, previously treated with cCRT were identified (Table 1). The primary tumors of two patients with distant metastases were included in the study, while the secondary lesions were not.

The mean treatment period was 47.5 days  $\pm$  4.0 days (range: 40–54 days). All patients were treated on a linear accelerator (VersaHD, Elekta AB, Stockholm, Sweden) with 10MV volumetric modulated arc therapy (VMAT). Treatment planning CTs (pCTs) and all dose deliveries were performed using a computer-controlled DIBH for target immobilization (ABC (Active Breathing Coordinator, Elekta AB, Sweden): 6, Catalyst (Catalyst, C-RAD, Sweden): 7). Therefore we did not consider an ITV but define GTV-PTV margins (axial: 10 mm, inferior-superior: 15 mm) [31]. For each patient, daily kV-based CBCT (XVI 5.0, Elekta AB, Sweden) scans were acquired for patient positioning. These scans were also obtained in multiple breath-hold-phases (“stop-and-go” breath-hold-only approach), immediately prior every treatment.

### Study image data preparation

The CBCT scans were reconstructed, rigidly registered to the pCTs using the clinically used registrations, in

**Table 1** Patient characteristics

Patient	Sex	Age	Tumor staging				Primary GTV (cm <sup>3</sup> )	Subtype	Tumor location	D <sub>presc</sub> (Gy)/fx
			T	N	M	Stage				
P1	m	70	T4	N0	M1	IVA	81.7	SCC	RML	60/30
P2	m	60	T4	N3	M0	IIIC	50.3	SCC	LLL	60/30
P3	m	83	T3	N3	M0	IIIC	29.9	SCC	RUL	60/30
P4	m	59	T3	N1	M0	IIIA	15.4	AC	RLL	60/30
P5	f	55	T4	N3	M0	IIIC	163.8	AC	RUL	60/30
P6	m	80	T4	N3	M0	IIIC	83.2	SCC	LUL	58/29
P7	m	80	T4	N0	M0	IIIA	165.8	SCC	LUL	60/30
P8	m	73	T3	N3	M0	IIIC	32.5	SCC	RUL	60/30
P9	f	69	T4	N2	M0	IIIB	312.1	SCC	RUL	60/30
P10	m	50	T4	N2	M1	IVA	82.4	SCC	RUL	60/30
P11	m	65	T4	N2	M0	IIIB	231.2	SCC	LUL	60/30
P12	m	71	T3	N3	M0	IIIC	116.6	AC	LML	56/28
P13	f	65	T4	N3	M0	IIIC	83.9	AC	RUL	60/30
		67.7 ± 9.6 (49–80)					111.4 ± 83.0 (15.4–501.9)			

The patient, tumor and fractionation characteristics are presented, where f = female, m = male, GTV = gross target volume, SCC = squamous cell carcinoma, AD = adenocarcinoma, LLL = left lower lobe, RLL = right lower lobe, LML = left middle lobe, RML = right middle lobe, LUL = left upper lobe, RUL = right upper lobe, D<sub>presc</sub> = prescription dose and fx = number of fractions. Tumors were staged according to the AJCC TNM staging system version 8. The average of the age and primary GTV size is displayed as mean ± standard deviation (ranges)

which a tumor match was favored and exported with a slice thickness of 3 mm to the treatment planning system (Monaco 5.11, Elekta). These CBCTs were converted into sCTs in a dedicated research software (ADMIRE, Elekta). For sCT generation this software utilizes a pre-trained artificial neural network [22]. Retrospectively, an expert physician contoured the GTV, heart, lungs, esophagus, spinal cord (sc), and the patient outline on the sCTs of the first fractions (sCT<sub>1</sub>) for all patients. These structures were deformably registered in an unsorted manner from the sCT<sub>1</sub> of a patient to the remaining sCTs (sCT<sub>2–n</sub>) of the patient using deformable image registration (DIR). The deformed structures were retrospectively reviewed and corrected for all sCTs of every patient, if necessary, by the same expert physician. The same window and level settings were used for correcting all structures in all sCTs of the same patient, respectively. An additional structure ipsilateral lung minus GTV (lung<sub>ipsilateral</sub>) was created for all sCTs. According to the clinical protocol all PTV<sub>2–n</sub> were generated out of the GTV<sub>2–n</sub> with GTV-PTV margins of 10 mm in axial and 15 mm in inferior-superior directions. These margins were used unaltered throughout the study and are in agreement with the margins which were used in the RTOG-0617 study protocol [5].

#### Treatment planning and dosimetric analysis

Initial VMAT treatment plans were generated in a Monte Carlo based treatment planning system (Monaco 5.11, Elekta) with a grid spacing of 3 mm and

a statistical uncertainty of 1% per dose calculation. Dosimetric constraints for inverse treatment planning were: V<sub>20Gy</sub>(lung<sub>ipsilateral</sub>) ≤ 37%, V<sub>20Gy</sub>(lung<sub>total</sub>) ≤ 30%, ipsilateral mean lung dose (MLD<sub>ipsilateral</sub>) ≤ 20 Gy, V<sub>5Gy</sub>(heart) as low as possible, V<sub>35Gy</sub>(heart) < 10%, mean heart dose (MHD) < 10 Gy, D<sub>0.1%</sub>(sc) < 50.5 Gy and the mean esophagus dose (MED) < 34 Gy, while 95% of the PTV should be covered with the prescription dose (D<sub>presc</sub>). Except for the heart the dosimetric constraints were adopted from RTOG-0617 [5]. The tolerance doses of the heart were further reduced, because V<sub>5Gy</sub>(heart), V<sub>35Gy</sub>(heart), and MHD are potentially associated with cardiac events [23, 32, 33]. All treatment plans were clinically accepted for patient treatment and optimized for maximum dose conformality.

The initial treatment plan of each patient was recalculated with identical control point settings, grid size, statistical uncertainty, and an isocenter which resulted from the image registration process onto sCT<sub>2–n</sub>. Assuming only interfractional and neglecting residual intrafractional motion in DIBH [34] this scenario represents the daily delivered dose to the patient with IGRT (IGRT scenario). For the two adaptation approaches, new treatment plans were re-optimized on sCT<sub>2–n</sub>. Therefore, a new isocenter was set in the center-of-mass of the daily PTVs. For the isoeffective scenario the ipsilateral lung constraints of the initial prescription template were iteratively reduced as long as the target coverage remained adequate. Each treatment plan was normalized to cover

95% of the actual  $PTV_{2-n}$  with  $D_{presc}$ . For the treatment plans of the isotoxic approach an equivalent procedure was applied with increasing the target dose. Subsequently, the  $V_{20Gy,2-n}(lung_{ipsilateral})$  was normalized to the initial treatment plan  $V_{20Gy,1}(lung_{ipsilateral})$  ... with a maximum normalization between 90% and 110%. For three patients, the lungs were cropped due to a reduced FOV in the CBCTs. For these patients, the absolute initial ipsilateral lung volume was taken for normalization. In addition, a maximum dose for the  $D_{95\%}(PTV)$  of 3.3 Gy per fraction was implemented in accordance with the 2.2–3.8 Gy of RTOG-1106 study protocol. Our lower maximal fractional dose of 3.3 Gy was chosen to preferably stay below the maximum total dose of 80.4 Gy of the RTOG-1106. Their study showed no adverse effects for this dose-escalation [35]. To avoid uncertainties due to a DIR-based dose accumulation, the resulting dose-volume histogram (DVH)-parameters of each fraction were evaluated independently. To enable using the standard DVH-parameters for cumulative dose distributions (like

$V_{20Gy}$ ) each fraction was evaluated with the total  $D_{presc}$ . Thus, the fractional dose limit of 3.3 Gy ( $D_{95\%}(PTV)$ ) corresponded to a limit of 100 Gy ( $D_{95\%}(PTV)$ ) in the total  $D_{presc}$ . In isotoxic cases where  $D_{95\%}(PTV) > 100$  Gy was feasible, the treatment plan was normalized, so that 100 Gy covered 95% of the PTV. The mean value of all fractions of each patient was considered as an estimation of the dose accumulation.

The dose distributions of all fractions were evaluated regarding the GTV and PTV coverage,  $V_{20Gy}(lung_{ipsilateral})$ ,  $MLD_{ipsilateral}$ ,  $MLD_{contralateral}$ , MHD,  $V_{5Gy}(heart)$ , MED, and the  $D_{0.1\%}(sc)$ . Furthermore, the equivalent dose in 2 Gy-fractions ( $EQD_2$ ) was determined using the linear quadratic model [36] with a specific tissue characterization ratio  $\alpha/\beta = 8.2$  Gy for the GTV and PTV [37]. The dosimetric parameters of the initial treatment plans were compared to the resulting plans of the IGRT, isoeffective, and isotoxic scenarios.

In Fig. 1 the dose distributions in the axial isocenter plane of the initial treatment plan (Fig. 1a) on  $sCT_1$  of a

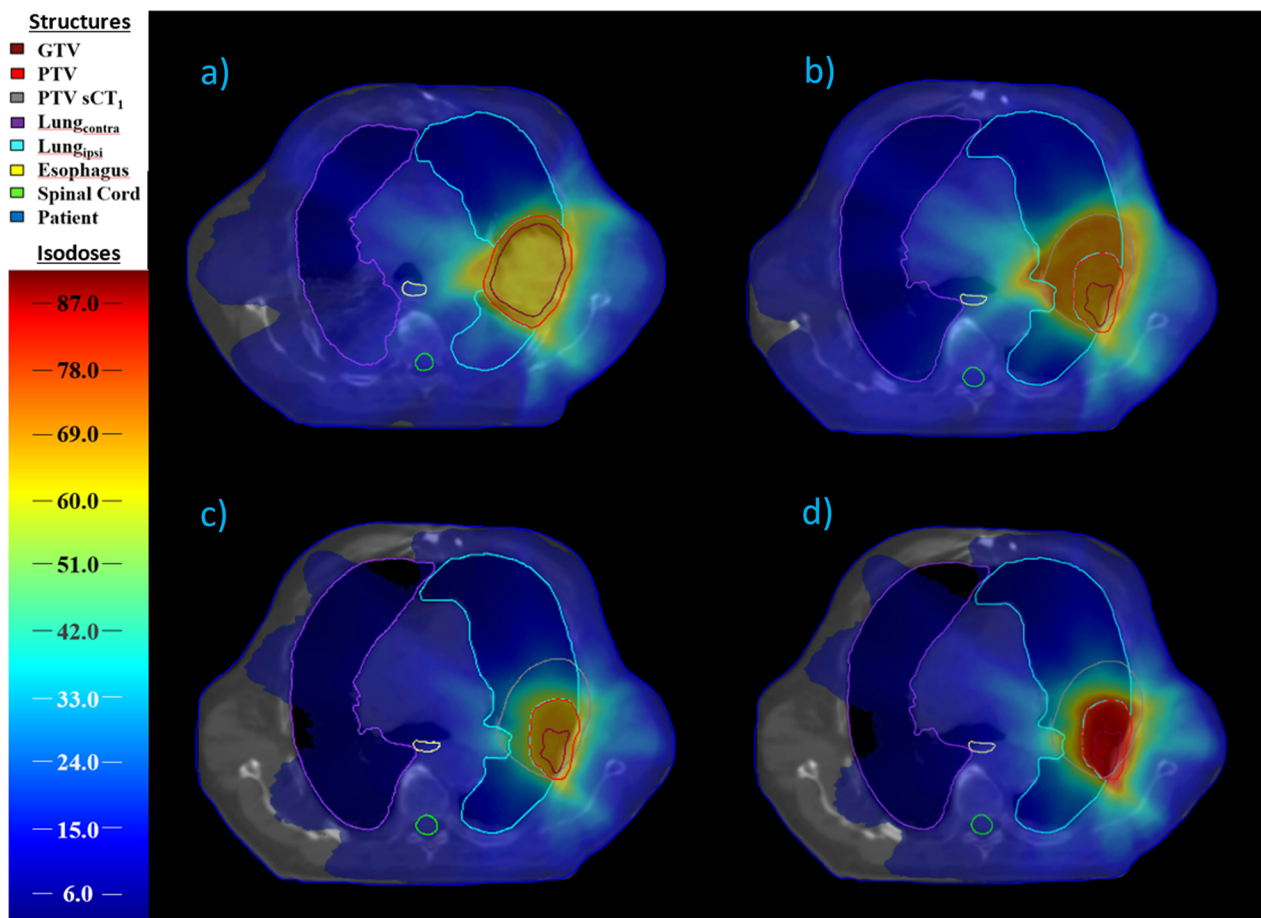


**Fig. 1** Exemplary dose distributions of a representative patient. Shown are dose distributions (a) of the original treatment plan, (b) of the last treatment fraction without adaptive radiotherapy (ART), (c) of an isoeffective ART, and (d) of an isotoxic ART treatment plan

representative patient is compared to the IGRT-, isoeffective- and isotoxic-dose distributions on  $sCT_{30}$ . One can see the regressed GTV in  $sCT_{30}$  (Fig. 1b–d).

### Statistical analysis

The aforementioned dose-volume relationships for IGRT, isoeffective and isotoxic ART approaches were compared to the initial treatment plan results and tested for statistically significant ( $p < 0.05$ ) differences using a non-parametric Wilcoxon signed-rank test in R (RStudio 1.4.1717, PBC, Boston, MA). Pearson's correlation coefficients (PCC) were determined to analyze potential correlations between GTV-regression and analyzed DVH-parameters.

### Ethics statement

This investigation was performed according to the principles of the Declaration of Helsinki and after Institutional Review Board (IRB) approval (2018-836R-MA). All data was anonymized prior to inclusion.

## Results

### GTV-regression

The mean decrease in GTV on the final  $sCT$ s was  $59.9\% \pm 15.8\%$  (range: 24.0–81.8%) compared with the initial GTV, corresponding to a mean reduction of  $1.4\% \pm 0.6\%$  per treatment fraction and  $0.9\% \pm 0.3\%$  per day (Fig. 2).

### Dosimetric analysis

The median DVH-parameters of the initial treatment plans and the three scenarios are presented in Table 2.

While the GTV-coverage remained intact in the IGRT scenario, the median  $D_{95\%}(PTV)$  was  $1.6 \text{ Gy} \pm 4.2 \text{ Gy}$  and the median  $EQD_2(D_{95\%}(PTV))$   $1.7 \text{ Gy} \pm 5.0 \text{ Gy}$  lower

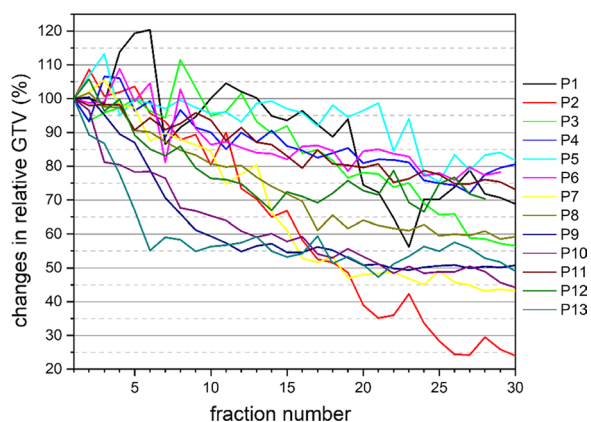


**Fig. 2** Daily volume changes of the gross target volume (GTV). Displayed are GTV dynamics for 13 patients (P1–P13) with locally advanced non-small cell lung cancer

than initially planned. The  $D_{95\%}(GTV)$  and  $D_{95\%}(PTV)$  were below 95% volume coverage in 21 (5.4%) and 108 (27.9%) fractions. Averaged over all treatment fractions of each patient the GTV and PTV coverage of 1 (7.7%) and 5 patients (38.5%) were too low, respectively. In the IGRT scenario all analyzed OAR-parameters were slightly higher than initially predicted. Compared to the initial treatment plan the median  $V_{20Gy}(\text{lung}_{\text{ipsilateral}})$ ,  $MLD_{\text{ipsilateral}}$ ,  $V_{5Gy}(\text{heart})$  and MHD were  $1.1\% \pm 4.4\%$ ,  $0.5 \text{ Gy} \pm 1.8 \text{ Gy}$ ,  $0.2\% \pm 6.7\%$ , and  $0.2 \text{ Gy} \pm 1.2 \text{ Gy}$  higher. The  $V_{20Gy}(\text{lung}_{\text{ipsilateral}})$ ,  $MLD_{\text{ipsilateral}}$  and the MHD were violating the previously mentioned constraints of 37%, 20 Gy, and 10 Gy in 69 (17.8%), 6 (1.6%), and 41 (10.6%) fractions and on average for 3 (23.1%), 0, and 1 patients (7.7%), while these tolerances were never exceeded in the initial treatment plans.

The PTV-coverage was restored in the isoeffective ART plans. The above-mentioned constraints for the  $D_{95\%}(GTV)$  and  $D_{95\%}(PTV)$  were not violated in any fraction in the isoeffective treatment plans. Simultaneously, the ipsilateral lung and heart were spared by  $3.1\% \pm 3.6\%$  (median  $V_{20Gy}(\text{lung}_{\text{ipsilateral}})$ ),  $1.4 \text{ Gy} \pm 1.3 \text{ Gy}$  (median  $MLD_{\text{ipsilateral}}$ ),  $2.9\% \pm 6.4\%$  (median  $V_{5Gy}(\text{heart})$ ), and  $0.5 \text{ Gy} \pm 1.4 \text{ Gy}$  (median MHD) compared to the initial plan. The OAR-sparing of the isoeffective approach is even more pronounced compared to the IGRT scenario with  $3.7\% \pm 6.9\%$  (median  $V_{20Gy}(\text{lung}_{\text{ipsilateral}})$ ),  $1.9 \text{ Gy} \pm 2.7 \text{ Gy}$  (median  $MLD_{\text{ipsilateral}}$ ),  $3.0\% \pm 5.7\%$  (median  $V_{5Gy}(\text{heart})$ ), and  $0.6 \text{ Gy} \pm 1.3 \text{ Gy}$  (median MHD). The constraints for the  $V_{20Gy}(\text{lung}_{\text{ipsilateral}})$ ,  $MLD_{\text{ipsilateral}}$  and the MHD were exceeded for 7 (1.8%), 0, and 13 (3.4%) fractions and on average for no patient, respectively.

In the dose-escalation scenario median dose-escalations of  $10.0 \text{ Gy} \pm 8.1 \text{ Gy}$  ( $D_{95\%}(GTV)$ ),  $12.4 \text{ Gy} \pm 10.3 \text{ Gy}$  ( $EQD_2(D_{95\%}(GTV))$ ),  $6.6 \text{ Gy} \pm 8.9 \text{ Gy}$  ( $D_{95\%}(PTV)$ ), and  $8.1 \text{ Gy} \pm 13.7 \text{ Gy}$  ( $EQD_2(D_{95\%}(PTV))$ ) were achieved. The aforementioned constraints for the  $D_{95\%}(GTV)$  and  $D_{95\%}(PTV)$  were violated in 0 and 12 (3.1%) cases, respectively. The constraints for the  $V_{20Gy}(\text{lung}_{\text{ipsilateral}})$ ,  $MLD_{\text{ipsilateral}}$  and the MHD were violated in 0, 7 (1.8%), and 27 (7.0%) fractions, respectively. In the accumulated dose no constraints were violated for any patients.

The IGRT scenario increased the median  $D_{0.1\%}(sc)$ , MED, and the  $MLD_{\text{contralateral}}$  compared with the initial TPs. In the two ART approaches these median DVH-parameters were lower compared with the IGRT scenario. The previously defined constraints ( $D_{0.1\%}(sc) < 50.5 \text{ Gy}$ ,  $MED < 34 \text{ Gy}$ ,  $V_{20Gy}(\text{lung}_{\text{total}}) \leq 30\%$ ) were not violated in any fraction of the three scenarios. The ipsilateral lung volume changes resulted in higher  $MLD_{\text{ipsilateral}}$ -doses in some fractions. That explains the higher maximal  $MLD_{\text{ipsilateral}}$ -doses in the IGRT, isoeffective, and isotoxic

**Table 2** DVH-parameters

Structure	Metric	Median ± Interquartile range (min—max)			
		Original treatment plan	IGRT	Isoeffective ART	Isotoxic ART
GTV	D <sub>95%</sub> (Gy)	60.5 ± 0.9 (59.0–62.3)	60.5 ± 2.0 (41.4–63.3)*	60.4 ± 1.6 (58.0–63.6)*	70.5 ± 9.4 (58.4–122.2)*
	Rel. D <sub>95%</sub> (%)	100.0	100.2 ± 1.4 (68.4–103.9)*	99.9 ± 1.9 (96.8–105.0)*	116.0 ± 13.5 (96.3–236.8)*
	EQD <sub>2</sub> (D <sub>95%</sub> ) (Gy)	60.6 ± 1.1 (58.8–62.8)	60.6 ± 2.4 (38.8–64.0)*	60.5 ± 1.9 (57.6–64.3)*	72.9 ± 11.9 (58.1–147.0)*
	Rel. EQD <sub>2</sub> (D <sub>95%</sub> ) (%)	100.0	100.3 ± 1.7 (64.1–104.7)*	99.9 ± 2.2 (96.1–106.0)*	119.6 ± 17.0 (95.4–234.0)*
PTV	D <sub>95%</sub> (Gy)	60.0 ± 0.0 (56.0–60.0)	57.9 ± 5.8 (16.4–62.1)*	60.0 ± 0.0 (55.8–60.2)	65.5 ± 8.1 (53.5–100.0)*
	Rel. D <sub>95%</sub> (%)	100.0	97.1 ± 7.3 (27.4–104.9)*	100.0 ± 0.1 (99.8–100.2)	109.2 ± 12.0 (94.2–221.3)*
	EQD <sub>2</sub> (D <sub>95%</sub> ) (Gy)	60.0 ± 0.1 (56.0–60.0)	58.7 ± 6.8 (14.1–62.5)*	60.0 ± 0.0 (55.8–60.2)	66.4 ± 9.8 (52.3–113.1)*
	Rel. EQD <sub>2</sub> (D <sub>95%</sub> ) (%)	100.0	98.8 ± 8.6 (23.5–105.9)*	100.0 ± 0.1 (99.8–100.3)	110.6 ± 14.8 (92.3–188.6)*
Lung <sub>ipsilateral</sub>	MLD (Gy)	14.2 ± 2.4 (7.8–16.9)	14.7 ± 3.0 (7.7–21.8)*	12.3 ± 3.4 (6.6–17.7)*	13.8 ± 2.5 (7.3–20.6)*
	Rel. MLD (%)	100.0	103.6 ± 12.7 (23.5–105.9)*	92.8 ± 10.6 (99.8–100.3)*	99.2 ± 3.4 (92.3–188.6)*
	V <sub>20Gy</sub> (%)	30.2 ± 12.3 (13.0–36.9)	31.3 ± 10.0 (12.7–48.8)*	26.6 ± 14.6 (10.7–40.7)*	30.2 ± 12.4 (13.0–37.0)
	Rel. V <sub>20Gy</sub> (%)	100.0	105.2 ± 14.7 (74.1–141.8)*	90.7 ± 14.4 (67.9–116.3)*	100.0 ± 0.0 (99.6–100.3)
Lung <sub>contralateral</sub>	MLD (Gy)	6.2 ± 4.4 (3.0–12.9)	6.7 ± 4.8 (2.7–13.7)*	6.0 ± 4.9 (2.2–12.9)*	6.5 ± 4.9 (2.6–13.6)*
	Rel. MLD (%)	100.0	105.1 ± 13.9 (88.1–150.1)*	96.7 ± 10.8 (71.6–124.3)*	102.7 ± 17.6 (73.7–146.8)*
Heart	MHD (Gy)	6.2 ± 5.0 (0.8–9.4)	6.3 ± 5.3 (0.8–15.0)*	5.8 ± 5.4 (0.55–13.0)*	6.2 ± 5.6 (0.8–14.0)*
	Rel. MHD (%)	100.0	100.0 ± 32.7 (53.6–257.2)*	90.4 ± 20.1 (49.0–164.8)*	100.0 ± 30.1 (46.4–196.1)*
	V <sub>5Gy</sub> (%)	34.7 ± 24.4 (9.3–59.1)	34.8 ± 26.4 (6.8–100.0)*	30.0 ± 21.7 (4.4–100.0)*	30.8 ± 20.7 (4.5–100.0)*
	Rel. V <sub>5Gy</sub> (%)	100.0	100.5 ± 23.6 (53.8–187.3)*	90.7 ± 19.3 (48.3–169.3)*	93.0 ± 29.7 (55.3–180.4)*
Esophagus	MED (Gy)	11.9 ± 9.4 (4.0–24.7)	12.5 ± 11.6 (2.9–27.5)*	11.0 ± 10.5 (2.9–25.7)*	11.1 ± 9.4 (2.7–25.1)*
	Rel. MED (%)	100.0	102.7 ± 16.1 (51.3–134.6)*	97.2 ± 17.6 (32.0–130.1)*	96.5 ± 22.3 (35.7–147.6)*
Spinal Cord	D <sub>0.1%</sub> (Gy)	20.3 ± 6.1 (11.3–26.1)	21.3 ± 5.9 (10.6–37.6)*	20.4 ± 6.4 (8.8–29.8)*	21.2 ± 6.8 (7.8–31.0)*
	Rel. D <sub>0.1%</sub> (%)	100.0	105.1 ± 11.1 (84.7–209.8)*	102.1 ± 15.3 (66.1–140.3)*	104.8 ± 16.1 (68.3–188.1)*

The absolute and relative median values of the DVH-parameters ± Interquartile ranges as well as (minimum-, maximum doses) for the gross target volume (GTV), planning target volume (PTV) and organs at risk are presented for the dose distributions of the following scenarios: original treatment plan (sCT<sub>1</sub>), after IGRT (sCT<sub>1-n</sub>), with isoeffective ART (sCT<sub>1-n</sub>), with isotoxic ART (sCT<sub>1-n</sub>). The abbreviations EQD<sub>2</sub>, MLD, MHD and MED are short for the equivalent dose in 2 Gy-fractions, mean lung dose, mean heart dose and mean esophagus dose, respectively. Statistically significant differences to the initial treatment plans are marked with an asterisk (\*)

scenarios. Higher maximum doses for the V<sub>5Gy</sub>(heart) and MHD in the three scenarios were caused by GTV movements towards the heart in 2 patients.

#### DVH-parameter correlation with GTV-regression

A PCC between the GTV-volume and a DVH-parameter ≥ ±0.5, which indicates an at least moderately strong

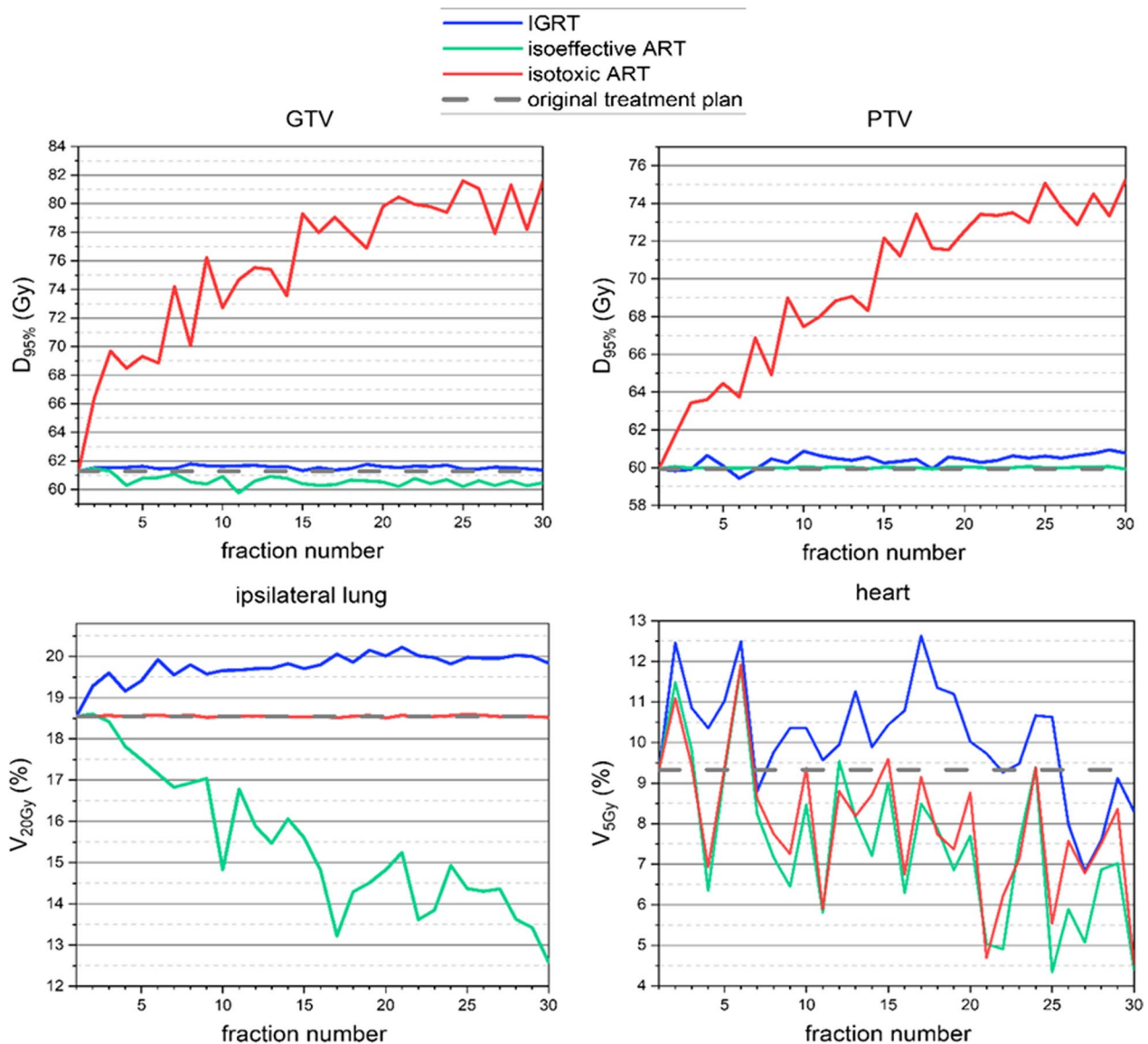


**Fig. 3** Fraction-wise analysis of dose-volume histogram (DVH)-parameters of a representative patient. The DVH-parameters of the gross target volume (GTV) ( $D_{95\%}(GTV)$ ), planning target volume (PTV) ( $D_{95\%}(PTV)$ ), ipsilateral lung ( $V_{20Gy}(lung_{ipsilateral})$ ) and the heart ( $V_{5Gy}$  (heart)) are shown as a function of treatment fractions for the three scenarios - without adaptive radiotherapy (ART) (blue), isoeffective ART (green), and isotoxic ART (red). The dashed grey line represents the respective DVH-parameter of the initial treatment plan

correlation, was found for the  $V_{20Gy}(lung_{ipsilateral}) = -0.6$  in the IGRT scenario. This indicates that a decreasing GTV-volume leads to an increase in ipsilateral lung-dose with IGRT-only. For the isoeffective scenario, on the other hand, the PCC of  $V_{20Gy}(lung_{ipsilateral})$  was  $+0.6$  which implies a decrease of ipsilateral lung-dose with a decrease in GTV-volume. In the isotoxic scenario with a PCC of the  $D_{95\%}(GTV) = -0.5$ , an increasing GTV-dose with decreasing GTV-volume was observed.

**Fraction-wise analysis of a representative patient**

Fraction-wise dosimetric analysis of the  $D_{95\%}(GTV)$ ,  $D_{95\%}(PTV)$ ,  $V_{20Gy}(lung_{ipsilateral})$ , and  $V_{5Gy}$ (heart) over all treatment fractions of one representative patient (with median GTV-reduction) with  $D_{presc} = 60$  Gy is presented in Fig. 3. In the last sCT of this patient, the GTV-volume was reduced to 59.3% of the initial GTV. The mean  $D_{95\%}(PTV)$  was 69.8 Gy in the isotoxic scenario, whereas in the isoeffective scenario the mean

$V_{20\text{Gy}}(\text{lung}_{\text{ipsilateral}})$  was reduced by 3.0%. One can see the aforementioned dose-escalation ( $D_{95\%}(\text{GTV})$  and  $D_{95\%}(\text{PTV})$ ) and the lung-dose sparing ( $V_{20\text{Gy}}$ ) in the isotoxic and isoeffective scenario, respectively. For the  $V_{5\%}(\text{heart})$  a strong fluctuation is noticeable in every scenario. In the IGRT scenario an increase in  $V_{20\text{Gy}}(\text{lung}_{\text{ipsilateral}})$  by 1.6% was found while the target coverage remained intact over all fractions.

## Discussion

To our knowledge, this is the first study evaluating the dosimetric benefits of daily isotoxic and isoeffective ART approaches for patients with stage III NSCLC on daily CBCT-based sCTs. The generated sCTs have the advantage of preserving the daily anatomy and providing accurate electron density allocations, comparable to those of the pCTs. While dosimetric errors were reported to be typically less than 1% with this method [22], the errors were further minimized by comparing dosimetric results to treatment plans optimized on the sCT<sub>1</sub> and not pCTs.

Dose accumulation is mostly based on deformation vector fields (DVF) generated with a DIR. The accuracy of this method depends strongly on the image resolution, artifacts, and image distortion [38, 39]. Furthermore, the generation of the DVFs is a problem with no unique solution due to too many degrees of freedom [40]. This eventually results in dose inaccuracy in DIR-based dose accumulation [39]. This inaccuracy becomes more pronounced for regressing structures because their mass is not preserved [41, 42]. That makes dose accumulations challenging when shrinking tumors are included [41, 42]. Zhong et al. reported a reduced MLD by around 2 Gy for isoeffective ART of patients with NSCLC from 17.3 Gy to either 15.2 Gy, 14.5 Gy or 14.8 Gy when using three different DIR algorithms for the same data. That yields an algorithm-based MLD fluctuation of 0.7 Gy (4%) between the three DIR algorithms [42].

Without adaptation, the GTV-coverage remained adequate, but the median  $D_{95\%}(\text{PTV})$  decreased by  $1.6 \text{ Gy} \pm 4.2 \text{ Gy}$ . In a study by Luo et al. in which the treatment plans of 24 NSCLC patients were retrospectively recalculated on weekly CBCTs, only 81.5% of the PTVs received the  $D_{\text{presc}}$  instead of 95.6% of the initial plans [43]. The evaluated OAR-doses were exceeded for all analyzed DVH-parameters. Since the known OAR tolerances are today solely based on the initial treatment plans [44], OAR tolerances are likely to change for ART. The analysis of Hoegen et al. yielded a lung dose increase (MLD,  $V_{20\text{Gy}}$ ) for 10 patients with NSCLC by daily recalculation on CBCTs without plan adaptations comparable to the results of this work [45].

## Benefits of isoeffective ART

In isoeffective ART, treatment plan adaptations to the regressed tumor volume allowed a restoration of the PTV coverage while minimizing the OAR-doses. The median MLD<sub>ipsilateral</sub> and  $V_{20\text{Gy}}(\text{lung}_{\text{ipsilateral}})$  were  $1.4 \text{ Gy} \pm 1.3 \text{ Gy}$  and  $3.1\% \pm 3.6\%$  lower than initially planned. In the study of Hoegen et al. with weekly isoeffective plan adaptations for 10 patients with NSCLC, this effect is less evident, which can be explained by less frequent adaptations [45]. Guckenberger et al. obtained weekly CT for 13 patients with NSCLC to simulate ART. At week 3 or 5, or both, the treatment plans were adjusted. The results of their isoeffective ART at weeks 3 and 5 were comparable to our results for MLD. The effect that they achieved similar results with only 2 adaptations could be due to larger mean GTV-volumes and higher GTV-regression rates in their patient collective [46].

In a recent retrospective study, an isoeffective ART group had a 4.3 Gy lower median MLD and 3.6 Gy lower median MHD than a non-ART group. It is of notice that this group in contrast to our study used smaller margin sizes for the ART group, which explains the large MLD and MHD sparing [24]. Despite their retrospective nature, these results demonstrate the possibilities of isoeffective ART. Only 20%, 7%, and 0.4% of the patients in the ART group experienced pneumonitis with a grade  $\geq 2$ ,  $\geq 3$ , or lethal instead of 50%, 21%, and 6% of the patient population without ART. The OS and PFS after two years increased by 13% and 8% in the ART group compared to the non-ART control group, respectively [24]. In this study, new 4D-CTs for each adaptation were required. If CBCTs, which are already used for patient positioning, or CBCT-based sCTs could be used for the treatment plan adaptation, the extra dose of the 4D-CTs could be avoided.

In some treatment fractions the OAR-constraints were violated due to tumor movement towards the heart and lung in two patients. Furthermore, lung volume changes caused higher  $V_{20\text{Gy}}$  of the ipsilateral lung in some fractions. To gain the initial coverage, the OAR doses were exceeded in the isoeffective ART scenario.

## Benefits of isotoxic ART

It is still a matter of discussion which patients could benefit from an isotoxic ART approach with a target dose-escalation and which upper dose limits are appropriate. Improved outcomes in dose-escalation studies for patients who received RT alone or after inducing chemotherapy up to 84 Gy [47] and 103 Gy [26] were found. Ramroth et al. showed a prolonged median survival with dose-escalation for patients without chemotherapy

in a meta-analysis involving 3795 patients from 25 trials. The time-corrected EQD<sub>2</sub> ranged from 36.4 Gy to 80.8 Gy. With cCRT the opposite occurred which might be due to higher levels of toxicity [48]. In the study trial RTOG-0617 patients with cCRT who were treated with a D<sub>presc</sub> of 60 Gy had better OS rates than patients who were treated with 74 Gy [5]. Schild et al. showed the more frequent occurrence of adverse events grade III or greater with dose-escalation in a meta-analysis involving 3600 patients from 16 trials [49]. Different to the RTOG-0617 and the study of Schild et al. for the isotoxic ART scenario, a fractional dose-escalation was chosen in this work to avoid tumor repopulation due to treatment prolongation [11, 50, 51] and the OAR-doses should not exceed the initially planned values to avoid the increased occurrence of adverse events.

The median D<sub>95%</sub>(GTV) was 10.0 Gy ± 8.1 Gy higher compared to the initial plans. That is a larger dose increase than the result of the isotoxic ART in the prior mentioned study by Guckenberger et al. with a mean escalation of the D<sub>95%</sub>(GTV) by 5.7 Gy. Remarkably, this dose-escalation was achieved by adapting only twice in the treatment period [46]. The median EQD<sub>2</sub>(D<sub>95%</sub>(PTV)) was 8.1 Gy ± 13.7 Gy higher than the initial treatment plans. That is lower than the mean EQD<sub>2</sub>(D<sub>95%</sub>(PTV)) dose-escalation of 13.4 Gy which was obtained by Weiss et al. by adapting treatment plans of 10 patients with NSCLC in weeks 2 and 4. That they achieved a higher dose-escalation with only 2 adaptations might be explainable by our dosimetric limit of the D<sub>95%</sub>(PTV), the larger GTV-reduction they reported, the chosen α/β-ratio, and furthermore, they escalated the dose until the MLD exceeded the initial dose by 1 Gy [52]. The ongoing RTOG-1106 study compares normofractionated patients with patients for whom a mid-treatment PET-CT was used for individualized dose-escalation. The median target dose with one adaptation was 71 Gy. The 2-year in-field local–regional control and primary tumor control of the patients in the adaptation arm was 10.7% and 17.1% higher than for the normofractionated patients [35]. An adaptation based on a PET-CT to the residual active volume might lead to more promising results, but is time-consuming and leads to additional doses which cannot be neglected and therefore, are unsuitable for daily adaptations [45, 53].

The normalization of the isotoxic ART treatment plans to the V<sub>20Gy</sub> of the ipsilateral lung could lead to an excess of the remaining DVH parameters in cases where the V<sub>20Gy</sub> was not the limiting OAR-constraint. Furthermore, we allowed dose normalization ratios between 90% and 110%, which could also cause a violation of OAR constraints in the isotoxic ART scenario.

### Limitations and benefits of the proposed approach

Having one physician performing all image segmentation reduces possible bias introduced by inter-individual assessments. Furthermore, contouring retrospectively in an unsorted sCT-order minimized a potential bias in favour of any method. Nevertheless, the volume changes of the GTV seen in Fig. 2 cannot be solely attributed to daily changes in tumor size, but could also be influenced by the resolution of the sCT and intraobserver variability of the structure delineation, which, however, is already covered by the GTV-PTV margin. Furthermore, accurate image segmentation of the heart was expected to be challenging since it is mostly located at the periphery of CBCT scans, where soft tissue discrimination is weak. Therefore, dosimetric consequences in this structure will be more likely prone to errors. Daily fluctuations of certain DVH-parameters as displayed in Fig. 3 demonstrate the difficulty of a reproducible treatment scenario and subsequent image segmentation. Especially daily fluctuations in the structure which is used for dose normalization (PTV or ipsilateral lung) will lead to dosimetric deviations. This is of particular interest when adaptations are performed on a regular but not daily basis, e.g. once weekly [28].

The relatively small FOV of conventional CBCT scanners resulted in only partially visible lungs for three patients. A larger FOV would be advantageous but might imply higher imaging doses.

Although daily ART becomes feasible with modern linear accelerators it is typically still time-consuming. The benefit of ART decreases from midterm to weekly and daily ART [28]. Woodford et al. stated that a tumor regression of at least 30% after 20 treatment fractions is worth replanning. A predictor of the time points for every patient, where the replanning is worth the effort or a predictor for OAR toxicities would be beneficial. This however, implies that pre-treatment volume images are available with a sufficiently high image quality.

Changes in the fractional dose of the isotoxic treatment plans could affect the patient's anatomy differently than the normofractionated ones. Higher fractional doses could further increase the effect of the GTV-regression and therefore, as well of the dose-escalation [42]; nonetheless, fractionation-related effects remain yet uncertain. In addition, the tested ART strategies are pre-treatment adaptations, which address only interfractional and not intrafractional anatomic changes, thus the effect is larger than that of offline ART strategies, but could underestimate the effect of real-time online ART Strategies.

Our approach for two different treatment strategies namely, isoeffective ART and isotoxic ART was feasible,

confirmed by an accurate dosimetric analysis of daily ART. All treatment plans were calculated for the same patient collective which makes them reproducible. In the isoeffective scenario the OAR-doses were spared with adequate target-coverage in all treatment fractions. In the isotoxic treatment plans the dose to the target volume could be escalated without relevantly increasing the OAR exposure.

### Potential future implementations

sCT-guided ART can be implemented on conventional linear accelerators that are equipped with a CBCT scanner. However, a separate CBCT to sCT conversion algorithm might need to be trained for different CBCT scanners [22]. Alternatively, some of the new linear accelerators, such as the Ethos (Varian Medical Systems, Palo Alto, CA), are already equipped for online ART [54].

Other possibilities are adaptations based on PET-CT or CT, which, however, are associated with additional radiation exposure [45, 53], or MR-guided adaptations. The advantages of adapted MR-guided radiotherapy are that MR imaging is possible without ionizing radiation [55, 56], MR images have a better soft tissue contrast than in CT, which facilitates delineation of the OAR and the target [57–60], and MR-guided ART allows for real-time monitoring [58, 61] and can be combined with functional imaging to assess tumor response to therapy. This offers the possibility to adjust the therapy based on the biological information [58]. The disadvantages of MR-guided ART are the low availability of MR linacs [62], the required manpower that has to be present during the entire treatment [60], and the treatment duration [61–63].

### Conclusion

Lung-IGRT results in appropriate interfractional target-coverage, at expenses of higher OAR exposure. Both online isoeffective and isotoxic ART achieve adequate OAR-sparing dosimetry, whereas the latter allows dose-escalated PTV coverage. Ongoing research will elucidate the clinical applicability of this approach.

### Acknowledgements

The authors would like to thank Gustav Meedt, Nicolette O'Connell, Peter Voet and Jiaofeng Xu from Elekta AB for their continuous support of this project.

### Author contributions

L.H. and J.F. conceived the study and prepared the manuscript. L.H. and C.S.K. exported datasets, generated sCTs and treatment plans and evaluated the results. The structures were delineated by G.R.S. J.B., V.S., M.E., F.A.G. and J.F. contributed intellectually to the manuscript and critically reviewed it. All authors read and approved the final manuscript.

### Funding

Open Access funding enabled and organized by Projekt DEAL. The project was partially funded by an Elekta AB research grant. The research software ADMIRE was provided by Elekta in a research version of Monaco.

### Availability of data and materials

The datasets used and analysed during the current study are available from the corresponding author on reasonable request.

### Declarations

#### Ethics approval

This investigation was performed according to the principles of the Declaration of Helsinki and after IRB approval (2018-836R-MA). All data was anonymized prior to inclusion.

#### Consent for publication

Not applicable.

#### Competing interests

The authors declare that they have no competing interests.

Received: 30 September 2022 Accepted: 6 February 2023

Published online: 22 February 2023

### References

1. Sonke JJ, Aznar M, Rasch C. Adaptive radiotherapy for anatomical changes. *Semin Radiat Oncol*. 2019;29(3):245–57.
2. Yamamoto T, et al. Changes in regional ventilation during treatment and dosimetric advantages of CT ventilation image guided radiation therapy for locally advanced lung cancer. *Int J Radiat Oncol Biol Phys*. 2018;102(4):1366–73.
3. Sonke JJ, Belderbos J. Adaptive radiotherapy for lung cancer. *Semin Radiat Oncol*. 2010;20(2):94–106.
4. Speirs CK, et al. Heart dose is an independent dosimetric predictor of overall survival in locally advanced non-small cell lung cancer. *J Thorac Oncol*. 2017;12(2):293–301.
5. Bradley JD, et al. Standard-dose versus high-dose conformal radiotherapy with concurrent and consolidation carboplatin plus paclitaxel with or without cetuximab for patients with stage IIIA or IIIB non-small-cell lung cancer (RTOG 0617): a randomised, two-by-two factorial phase 3 study. *Lancet Oncol*. 2015;16(2):187–99.
6. Wang K, et al. Heart dosimetric analysis of three types of cardiac toxicity in patients treated on dose-escalation trials for stage III non-small-cell lung cancer. *Radiother Oncol*. 2017;125(2):293–300.
7. Appel S, et al. Image-guidance triggered adaptive replanning of radiation therapy for locally advanced lung cancer: an evaluation of cases requiring plan adaptation. *Br J Radiol*. 2020;93(1105):20190743.
8. Caglar HB, Othus M, Allen AM. Esophagus in-field: a new predictor for esophagitis. *Radiother Oncol*. 2010;97(1):48–53.
9. Kaymak-Cerkesli ZA, Ozkan EE, Ozseven A. The esophageal dose-volume parameters for predicting Grade I–II acute esophagitis correlated with weight loss and serum albumin decrease in lung cancer radiotherapy. *J Cancer Res Ther*. 2021;17(1):94–8.
10. Moller DS, et al. Heterogeneous FDG-guided dose-escalation for locally advanced NSCLC (the NARLAL2 trial): design and early dosimetric results of a randomized, multi-centre phase-III study. *Radiother Oncol*. 2017;124(2):311–7.
11. Ma L, et al. A current review of dose-escalated radiotherapy in locally advanced non-small cell lung cancer. *Radiol Oncol*. 2019;53(1):6–14.
12. Bradley JD, et al. Long-term results of NRG oncology RTOG 0617: standard-versus high-dose chemoradiotherapy with or without cetuximab for unresectable stage III non-small-cell lung cancer. *J Clin Oncol*. 2020;38(7):706–14.
13. Spigel DR, et al. Five-year survival outcomes from the PACIFIC trial: durvalumab after chemoradiotherapy in stage III non-small-cell lung cancer. *J Clin Oncol*. 2022;40(12):1301–11.
14. Benedict SH, et al. Stereotactic body radiation therapy: the report of AAPM Task Group 101. *Med Phys*. 2010;37(8):4078–101.
15. Lim-Reinders S, et al. Online adaptive radiation therapy. *Int J Radiat Oncol Biol Phys*. 2017;99(4):994–1003.
16. Moller DS, et al. Adaptive radiotherapy for advanced lung cancer ensures target coverage and decreases lung dose. *Radiother Oncol*. 2016;121(1):32–8.

17. Kaplan LP, et al. Cone beam CT based dose calculation in the thorax region. *Phys Imaging Radiat Oncol.* 2018;7:45–50.
18. Giacometti V, Hounsell AR, McGarry CK. A review of dose calculation approaches with cone beam CT in photon and proton therapy. *Phys Med.* 2020;76:243–76.
19. Schröder L, et al. Evaluating the impact of cone-beam computed tomography scatter mitigation strategies on radiotherapy dose calculation accuracy. *Phys Imaging Radiat Oncol.* 2019;10:35–40.
20. Hansen DC, et al. ScatterNet: a convolutional neural network for cone-beam CT intensity correction. *Med Phys.* 2018;45(11):4916–26.
21. Jiang Y, et al. Scatter correction of cone-beam CT using a deep residual convolution neural network (DRCNN). *Phys Med Biol.* 2019;64(14):145003.
22. Eckl M, et al. Evaluation of a cycle-generative adversarial network-based cone-beam CT to synthetic CT conversion algorithm for adaptive radiation therapy. *Phys Med.* 2020;80:308–16.
23. Wang K, et al. Cardiac toxicity after radiotherapy for stage III non-small-cell lung cancer: pooled analysis of dose-escalation trials delivering 70 to 90 Gy. *J Clin Oncol.* 2017;35(13):1387–94.
24. Moller DS, et al. Survival benefits for non-small cell lung cancer patients treated with adaptive radiotherapy. *Radiother Oncol.* 2022.
25. Vivekanandan S, et al. The impact of cardiac radiation dosimetry on survival after radiation therapy for non-small cell lung cancer. *Int J Radiat Oncol Biol Phys.* 2017;99(1):51–60.
26. Kong FM, et al. High-dose radiation improved local tumor control and overall survival in patients with inoperable/unresectable non-small-cell lung cancer: long-term results of a radiation dose escalation study. *Int J Radiat Oncol Biol Phys.* 2005;63(2):324–33.
27. Machtay M, et al. Higher biologically effective dose of radiotherapy is associated with improved outcomes for locally advanced non-small cell lung carcinoma treated with chemoradiation: an analysis of the Radiation Therapy Oncology Group. *Int J Radiat Oncol Biol Phys.* 2012;82(1):425–34.
28. Dial C, et al. Benefits of adaptive radiation therapy in lung cancer as a function of replanning frequency. *Med Phys.* 2016;43(4):1787.
29. Haslett K, et al. Isotoxic intensity modulated radiation therapy in stage III non-small cell lung cancer: a feasibility study. *Int J Radiat Oncol Biol Phys.* 2021;109(5):1341–8.
30. Kong FM, et al. RTOG0617 to externally validate blood cell ERCC1/2 genotypic signature as a radiosensitivity biomarker for both tumor and normal tissue for individualized dose prescription. *Int J Radiat Oncol Biol Phys.* 2020;108(3):52.
31. Boda-Heggemann J, et al. Deep inspiration breath hold-based radiation therapy: a clinical review. *Int J Radiat Oncol Biol Phys.* 2016;94(3):478–92.
32. Ning MS, et al. Incidence and predictors of pericardial effusion after chemoradiation therapy for locally advanced non-small cell lung cancer. *Int J Radiat Oncol Biol Phys.* 2017;99(1):70–9.
33. Atkins KM, et al. Cardiac radiation dose, cardiac disease, and mortality in patients with lung cancer. *J Am Coll Cardiol.* 2019;73(23):2976–87.
34. Vogel L, et al. Intra-breath-hold residual motion of image-guided DIBH liver-SBRT: an estimation by ultrasound-based monitoring correlated with diaphragm position in CBCT. *Radiother Oncol.* 2018;129(3):441–8.
35. Kong F-MS, et al. NRG-RTOG 1106/ACRIN 6697: a phase IIR trial of standard versus adaptive (mid-treatment PET-based) chemoradiotherapy for stage III NSCLC: results and comparison to NRG-RTOG 0617 (non-personalized RT dose escalation). *J. Clin. Oncol.* 2021; **39**(15\_suppl): 8548.
36. Loap P, Fourquet A, Kirova Y. The limits of the linear quadratic (LQ) model for late cardiotoxicity prediction: example of hypofractionated rotational intensity modulated radiation therapy (IMRT) for breast cancer. *Int J Radiat Oncol Biol Phys.* 2020;106(5):1106–8.
37. van Leeuwen CM, et al. The alpha and beta of tumours: a review of parameters of the linear-quadratic model, derived from clinical radiotherapy studies. *Radiat Oncol.* 2018;13(1):96.
38. Schultheiss TE, Tome WA, Orton CG. Point/counterpoint: it is not appropriate to “deform” dose along with deformable image registration in adaptive radiotherapy. *Med Phys.* 2012;39(11):6531–3.
39. Chetty IJ, Rosu-Bubulac M. Deformable registration for dose accumulation. *Semin Radiat Oncol.* 2019;29(3):198–208.
40. Amstutz F, et al. An approach for estimating dosimetric uncertainties in deformable dose accumulation in pencil beam scanning proton therapy for lung cancer. *Phys. Med. Biol.* 2021;66(10).
41. Zhong H, Chetty IJ. Caution must be exercised when performing deformable dose accumulation for tumors undergoing mass changes during fractionated radiation therapy. *Int J Radiat Oncol Biol Phys.* 2017;97(1):182–3.
42. Zhong H, et al. Evaluation of adaptive treatment planning for patients with non-small cell lung cancer. *Phys Med Biol.* 2017;62(11):4346–60.
43. Luo J, et al. Study of the cumulative dose between fractions of lung cancer radiotherapy based on CT and CBCT image deformable registration technology. *Front. Phys.* 2020; 8.
44. Marks LB, et al. Use of normal tissue complication probability models in the clinic. *Int J Radiat Oncol Biol Phys.* 2010;76(3 Suppl):S10–9.
45. Hoegen P, et al. Cone-beam-CT guided adaptive radiotherapy for locally advanced non-small cell lung cancer enables quality assurance and superior sparing of healthy lung. *Front Oncol.* 2020;10:564857.
46. Guckenberger M, et al. Potential of adaptive radiotherapy to escalate the radiation dose in combined radiochemotherapy for locally advanced non-small cell lung cancer. *Int J Radiat Oncol Biol Phys.* 2011;79(3):901–8.
47. Rosenzweig KE, et al. Results of a phase I dose-escalation study using three-dimensional conformal radiotherapy in the treatment of inoperable nonsmall cell lung carcinoma. *Cancer.* 2005;103(10):2118–27.
48. Ramroth J, et al. Dose and fractionation in radiation therapy of curative intent for non-small cell lung cancer: meta-analysis of randomized trials. *Int J Radiat Oncol Biol Phys.* 2016;96(4):736–47.
49. Schild SE, et al. Toxicity related to radiotherapy dose and targeting strategy: a pooled analysis of cooperative group trials of combined modality therapy for locally advanced non-small cell lung cancer. *J Thorac Oncol.* 2019;14(2):298–303.
50. Zehentmayr F, et al. Radiation dose escalation with modified fractionation schedules for locally advanced NSCLC: a systematic review. *Thorac Cancer.* 2020;11(6):1375–85.
51. McMillan MT, et al. Radiation treatment time and overall survival in locally advanced non-small cell lung cancer. *Int J Radiat Oncol Biol Phys.* 2017;98(5):1142–52.
52. Weiss E, et al. Dose escalation for locally advanced lung cancer using adaptive radiation therapy with simultaneous integrated volume-adapted boost. *Int J Radiat Oncol Biol Phys.* 2013;86(3):414–9.
53. Smith-Bindman R, et al. Radiation dose associated with common computed tomography examinations and the associated lifetime attributable risk of cancer. *Arch Intern Med.* 2009;169(22):2078–86.
54. Mao W, et al. Evaluation of auto-contouring and dose distributions for online adaptive radiation therapy of patients with locally advanced lung cancers. *Pract Radiat Oncol.* 2022;12(4):e329–38.
55. Ahmad SB, et al. Evaluation of a commercial MRI Linac based Monte Carlo dose calculation algorithm with GEANT4. *Med Phys.* 2016;43(2):894–907.
56. Randall JW, et al. Towards accurate and precise image-guided radiotherapy: clinical applications of the MR-Linac. *J Clin Med.* 2022; 11(14).
57. Kong FM, et al. Effect of Midtreatment PET/CT-adapted radiation therapy with concurrent chemotherapy in patients with locally advanced non-small-cell lung cancer: a phase 2 clinical trial. *JAMA Oncol.* 2017;3(10):1358–65.
58. Crockett CB, et al. Initial clinical experience of MR-guided radiotherapy for non-small cell lung cancer. *Front Oncol.* 2021;11:617681.
59. Schiff JP, et al. A pilot study of same-day MRI-only simulation and treatment with MR-guided adaptive palliative radiotherapy (MAP-RT). *Clin Transl Radiat Oncol.* 2023;39:100561.
60. Murray J, Tree AC. Prostate cancer: advantages and disadvantages of MR-guided RT. *Clin Transl Radiat Oncol.* 2019;18:68–73.
61. Botman R, et al. The clinical introduction of MR-guided radiation therapy from a RTT perspective. *Clin Transl Radiat Oncol.* 2019;18:140–5.
62. Garcia Schuler HI, et al. Operating procedures, risk management and challenges during implementation of adaptive and non-adaptive MR-guided radiotherapy: 1-year single-center experience. *Radiat Oncol.* 2021;16(1):217.
63. Henke LE, et al. Stereotactic MR-guided online adaptive radiation therapy (SMART) for ultracentral thorax malignancies: results of a phase 1 trial. *Adv Radiat Oncol.* 2019;4(1):201–9.

## Publisher's Note

Springer Nature remains neutral with regard to jurisdictional claims in published maps and institutional affiliations.